

1 *Type of the Paper (Article)*

2 **Evaluation of gridded multi-satellite precipitation 3 (TRMM-3B42-V7) estimation performance in the 4 Upper Indus Basin (UIB)**

5 **Asim Jahangir Khan^{1,2,*}, Manfred Koch¹ and Karen Milena Chinchilla¹**

6 ¹ Department of Geohydraulics and Engineering Hydrology, University of Kassel, Germany (Manfred Koch
7 - kochm@uni-kassel.de, manfred_kochde@yahoo.de); Karen Milena Chinchilla - chatiking@gmail.com -)

8 ² Department of Environmental Sciences, COMSATS Institute of Information Technology, Abbottabad
9 Campus.

10 * Correspondence: asimjkw@gmail.com; uk053114@student.uni-kassel.de; Tel.: +49-17631674283

11

12 **Abstract:** The present study aims to evaluate the capability of the TRMM-3B42-(V7) precipitation
13 product to estimate appropriate precipitation rates in the Upper Indus basin (UIB) and the analysis
14 of the dependency of the estimates' accuracies on the time scale. To that avail statistical analyses
15 and comparison of the TMPA- products with gauge measurements in the UIB are carried out. The
16 dependency of the TMPA estimates' quality on the time scale is analysed by comparisons of daily,
17 monthly, seasonal and annual sums for the UIB. The results show considerable biases in the TMPA-
18 (TRMM) precipitation estimates for the UIB, as well as high false alarms and miss ratios. The
19 correlation of the TMPA- estimates with ground-based gauge data increases considerably and
20 almost in a linear fashion with increasing temporal aggregation, i.e. time scale. The BIAS is mostly
21 positive for the summer season, while for the winter season it is predominantly negative, thereby
22 showing a slight over-estimation of the precipitation in summer and under-estimation in winter.
23 The results of the study suggest that, in spite of these discrepancies between TMPA- estimates and
24 gauge data, the use of the former in hydrological watershed modelling, endeavoured presently by
25 the authors, may be a valuable alternative in data- scarce regions, like the UIB, but still must be
26 taken with a grain of salt.

27 **Keywords:** Precipitation; Tropical Rainfall Measurement Mission (TRMM); Multi-satellite
28 Precipitation Analysis (TMPA); Upper Indus basin (UIB).

29

30 **1. Introduction**

31 The continued improvements in computation capabilities and the subsequent increase in the
32 development of spatially explicit and distributed models for expressing environmental phenomena
33 has necessitated the provision of more intensive and improved data for environmental variables both
34 in space and time. Two major issues, especially, in hydro-meteorological studies, are the possible
35 sparsity of data sampling points (gauge stations), and the discontinuities in the data and in the quality
36 of the temporal records. These issues are more frequent in mountainous regions with high altitudes
37 which are immensely challenging environments for measurements of precipitation, either through
38 remote-sensing or the traditional ground based methods, because of the difficult topography and the
39 highly variable weather and climatic conditions [1, 2]. Similarly, these and other reasons have
40 restricted many developing countries to have consistent spatial and temporal coverage for ground-
41 based precipitation measurements [2, 3] and make it difficult for them to achieve an effective spatial
42 coverage of rainfall [4, 5]. The consequent lack of good quality precipitation data, then turns out to
43 be a big hurdle for properly assessing impacts of climate change on water resources in these regions
44 [1].

45 As data with an acceptable gridded resolution of daily climatic variables are critical for
46 hydrological and water resources modeling [6, 7], managing the gaps in the data appropriately is
47 then the first stage of most climatological, environmental and hydrological studies [2]. This step is
48 also necessary to improve the spatial resolution for sparse gauge station data set, before using it as
49 an input for spatially-distributed rainfall-runoff models, because the gauge-based interpolation
50 methods, commonly used in hydrologic models, usually do not cover the spatial heterogeneity of the
51 variability of climatic variables in the catchment. These errors in the interpolated data field have then
52 the potential to significantly bias model calibrations and water balance calculations [6].

53 Fortunately, the continued scientific development is also showing new prospects in addressing
54 these issues. . For example, the advancements in the gathering and deriving climate data through
55 satellite remote sensing could provide a possible opportunity to mend some of the issues with regard
56 to the spatial coverage of climate data. That is why the use of satellite-based precipitation products,
57 individually, or in combination with land-based gauge data, has been increasingly recognized as a
58 very promising alternative to address the aforementioned problems [5]. Such precipitation products
59 prove to be of great value, especially, in developing countries with remote and high-altitude
60 locations, where conventional rain gauge- or weather data are of bad quality or have low coverage
61 [8][8].

62 There are numerous satellite-based precipitation products currently available with varying
63 degrees of accuracy. These include the Climate Prediction Center (CPC) morphing algorithm
64 (CMORPH) [9], the Global Satellite Mapping of Precipitation [10–12], the Naval Research Laboratory
65 Global Blended Statistical Precipitation Analysis [13] and the Tropical Rainfall Measuring Mission
66 (TRMM) Multisatellite Precipitation Analysis (TMPA) [14, 15] and a few others. Since their inception,
67 most of these gridded datasets have been evaluated for their suitability and usability for a specific
68 regions or intended uses. In general such investigations are specifically for mountainous regions, and
69 even less for the Hindu Kush, Karakoram and Himalays (HKH) region. In the HKH and the Upper
70 Indus Basin (UIB) region, most of the reported work related to evaluation of gridded precipitation
71 products, are suggestive of considerable biases in the gridded products in comparison to the gauge
72 records [16–19].

73 Additionally the quality, coverage or representativeness of the available observed gauge records
74 have also been questioned and sometimes regarded below par [20–22] with considerable under
75 estimation of regional precipitation amounts especially at higher altitudes (Khan and Koch unpublished).(the
76 spatial distribution of estimated real precipitation by khan and Koch (unpublished) over study are is given in
77 the supplementary materials – Appendix-I while the Vertical meteorological and cryospheric regimes in UIB
78 (modified from Hewitt 2007) is given in Appendix-II)

79 While, in most cases, these gridded global precipitation data sets are some interpolated version
80 of point measurements, (most often through geo-statistical procedures), they may only be useful for
81 regions where dense network of rain gauges are available, because otherwise, in absence of a dense
82 enough networks or over regions of complex topographies, the interpolated precipitation present a
83 very generalized destitution, not able to reflect on the prevalent orographic, surface or atmospheric
84 processes [19].

85
86 In comparison with the sparse gauge observations or the gridded data products, based on them,
87 satellite-based precipitation products, such as “Tropical Rainfall Measurement Mission” (TRMM)
88 “Multi-satellite Precipitation Analysis” (TMPA) (TRMM-3B42-(V7) have an inherent advantage, due
89 to their higher spatial coverage. However, they also have certain limitations, because they are indirect
90 estimates of rainfall, which depend on the cloud height and the properties of the cloud’s surfaces (IR-
91 algorithms) and on the integrated sparse and multi-source hydro-meteorological content (passive
92 microwave algorithms) [23, 15, 24]. Before such satellite-based data can be used with confidence, it is
93 therefore important to evaluate its accuracy or error characteristics by comparing it with data from
94 ground-based observations.

95
96 The current study was therefore aimed at assessing the skill of the TRMM precipitation dataset
97 in matching the magnitudes and occurrences, at different temporal scales, at all the points of the

98 observational network available, to evaluate its further processing and correction requirements or
99 suitability for subsequent use in hydrological modelling.

100 **2. Materials and Methods**

101 *2.1. Study Area: "The Upper Indus River Basin (UIB)*

102 The Indus River, one of the largest rivers in Asia with a total length of about 2880 km, has a
103 drainage area of about 912,000 km² which extends across portions of India, China, Pakistan and
104 Afghanistan. The portion of the Indus that comprises the upper Indus river basin (UIB), with a logical
105 lower boundary at Tarbela Dam, is about 1125 km long and drains an area of about 170,000 km² [25]
106 .

107 Being a high-mountain region, the UIB contains the largest area of perennial glacial ice cover (22
108 000 km²) outside the polar regions of the earth, and which extends even further during the winter
109 season [26]. The altitude within the UIB ranges from as low as 455 m to a height of 8611 m and, as a
110 result, the climate varies greatly within the basin [27].

111 The summer monsoon has no significant effect on the basin, as almost 90% of its area lies in the
112 rain shadow of the Himalayan belt [28][20]. Except for the south-facing foothills, the intrusion of the
113 Indian-ocean monsoon is limited by the mountains, so that its influence weakens northwestward.
114 Subsequently, the climatic controls in the UIB are quite different from that in the Himalayas on the
115 eastern side. In fact, over the extent of the UIB, most of the annual precipitation originates in the west
116 and falls in winter and spring, whereas occasional rains are brought by the monsoonal incursions to
117 the trans-Himalayan areas, but so that even during the summer months the trans-Himalayan areas
118 do not obtain all their precipitation from the monsoons [29–32].

119 Climatic variables are usually strongly influenced by topographic altitude. Several studies have
120 pointed out that precipitation in the HKH region exhibits large changes over short distances and has
121 a considerable vertical gradient [33–36, 30, 29]. Thus the northern valley floors of the UIB are arid,
122 with annual precipitation of only 100–200 mm, but these totals increase with elevation and reach upto
123 600 mm at 4400 m, and even reach to an annual glacier accumulation rates of 1500 to 2000 mm at
124 5500 m altitude, according to some glaciological studies [29]. The average snow cover area in the
125 Upper Indus River Basin fluctuate between ~10% to 70%. Snow cover in the area is at a maximum of
126 70–80% in the winter- (December to February) snow accumulation period and at a minimum 10–15%
127 in the summer- (June to September) snow melt period [27]. Stream flow is generated by the
128 combination of the storm runoff in the lower parts of the upper Indus basin and the snow- and glacier
129 runoff from the higher parts of the UIB [37, 25].

130

131

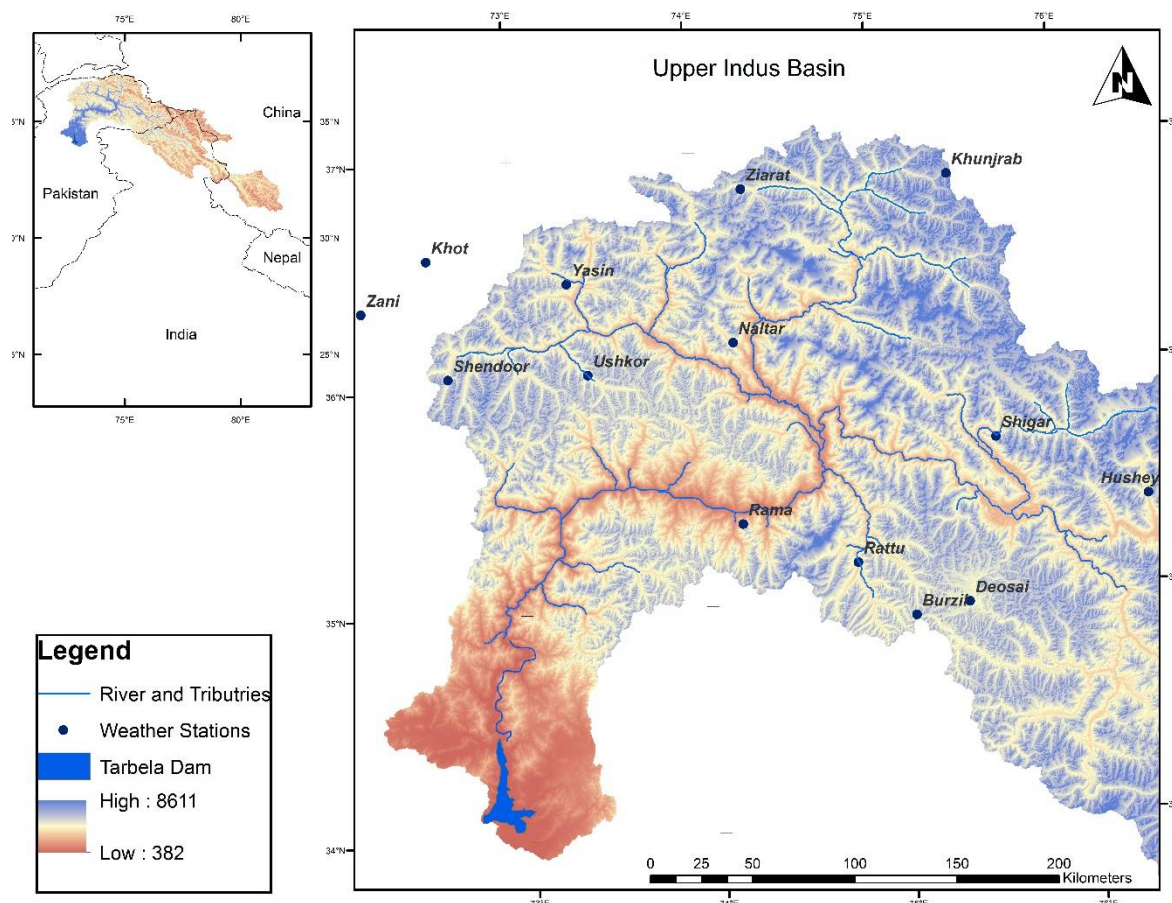


Figure 1: Upper Indus Basin with hydro-climatological stations

132 2.1.1. TMPA Data (TRMM 3B42 V7)

133 In this study the TRMM 3B42 (V7) precipitation product is used. This product is basically a
 134 calibration-based combination scheme for precipitation estimates from multiple satellites and space-
 135 borne sensors, including infrared, microwave, radar data and gauge measurements. Though the
 136 dataset has very good spatio-temporal resolution ($0.25^\circ \times 0.25^\circ$ grid, 3-hourly) and good global
 137 coverage (latitude band 50°N to 50°S) and is available since 1998 to the recent past [15, 1] it also has
 138 certain uncertainties, because the inputs on which they are based are indirect estimates of rainfall,
 139 depending on the cloud height and the properties of the cloud surface (IR algorithms) and on the
 140 integrated sparse and multi-source hydro-meteorological content (passive microwave algorithms)
 141 [15, 24, 14].

142 During the current study, 3-hourly data from January 1, 1998 to December 31, 2008, were
 143 summed to daily accumulated precipitation for each of the $0.25^\circ \times 0.25^\circ$ grid box, which have a gauge
 144 station, and evaluated for match with the corresponding gauge station's observed daily accumulated
 145 precipitation. As the observational network is scant, no TRMM grid box had more than one in situ
 146 gauge station located in it.

147 2.1.2. Observed gauge data

148 In HKH region of Pakistan, observed in situ data are limited, and operated by different
 149 organizations, mainly the Pakistan Meteorological Department (PMD) and Water and Power
 150 Development Authority (WAPDA). The stations operated by PMD have daily time step climate data
 151 available for longer periods (1947 to date) but with huge gaps and missing data in the record and
 152 with only monthly data available freely for research purposes. Furthermore, all the PMD stations are
 153 valley-based, at elevations below than 3000 m a.s.l. altitude, and therefore hardly represent the
 154 frequency and amount of precipitation in the high-altitude areas. The climate stations, operated by

155 WAPDA, are fairly new and have considerably consistent, data over the time period, coinciding with
 156 the TRMM product. These gauge stations are distributed almost evenly across the UIB inside Pakistan
 157 and cover a wide range of elevations. During the current study, daily precipitation records of 14
 158 meteorological stations operated by WAPDA were utilized for evaluation of TRMM estimates. Their
 159 geographical attributes are given in Table 1. The evaluation limited to the duration of 1998 to 2008,
 160 as the observed precipitation data could not be acquired for the period beyond 2008.

161 **Table 1;** Geographical attributes of the Precipitation gauge Network

	S. No.	Station name	Latitude (°)	Longitude (°)	Altitude (m)
High Altitude (2367-4440 m.a.s.l.) stations operated by Water and Power Development Authority, Pakistan (WAPDA)	1	Burzil	34.906	75.902	4030
	2	Deosai	35.09	75.54	4149
	3	Hushey	35.42	76.37	3075
	4	Khot	36.517	72.583	3505
	5	Khunjrab	36.84	75.42	4440
	6	Naltar	36.17	74.18	2898
	7	Rama	35.36	74.81	3179
	8	Rattu	35.15	74.8	2718
	9	Shendoor	36.09	72.55	3712
	10	Shigar	35.63	75.53	2367
	11	Ushkor	36.05	73.39	3051
	12	Yasin	36.454	73.3	3350
	13	Zani	36.334	72.167	3895
	14	Ziarat	36.77	74.46	3020

162 **2.2. Methods**

163 The quantitative comparison of the TRMM-estimates with ground rain-gauge station
 164 observations is done by employing various widely used statistical indicators. These include the
 165 correlation coefficient (R), the mean relative bias error ($rBIAS$), the mean bias error (MBE); mean
 166 absolute error (MAE), and the root mean square error ($RMSE$). The R , $rBIAS$, MBE , MAE and $RMSE$
 167 are defined in the following equations:

$$168 R = \frac{\sum_{i=1}^n (T_i - \bar{T})(G_i - \bar{G})}{\sqrt{\sum_{i=1}^n (T_i - \bar{T})^2} \sqrt{\sum_{i=1}^n (G_i - \bar{G})^2}} \quad (1)$$

$$169 rBIAS = \frac{1}{n} \sum_{i=1}^n \left(\frac{T_i - G_i}{\frac{1}{n} \sum_{i=1}^n G_i} \right) \quad (2)$$

170 $MAE \geq \frac{1}{n} \sum_{i=1}^n |T_i - G_i|$ (3)

171 $MBE \geq \frac{1}{n} \sum_{i=1}^n (T_i - G_i)$ (4)

172 $RMSE = \sqrt{\frac{1}{n} \sum_{i=1}^n (T_i - G_i)^2}$ (5)

173 where n is the number of samples, T_i are satellite-based precipitation, G_i are gauge-based
 174 precipitation, and \bar{T} and \bar{G} are the corresponding means. Among these statistical indices, R shows
 175 the degree of linear correlation between TRMM precipitation estimates and gauge observations;
 176 MBE , MAE and $rBIAS$ are used to assess the systematic bias, i.e. the deviation of the satellite
 177 precipitation from the gauge observations, and the $RMSE$ gives the magnitude of the average error
 178 in relative terms.

179 **Table 2.** Contingency table 2X2

		OBSERVED VALUES (GAUGE DATA)		TOTAL
		YES	NO	
ESTIMATED VALUES (TRMM-ESTIMATES)	YES	-a- Hits	-b- False Alarms	Total-Yes Estimated
	NO	-c- Misses	-d- Correct negative	Total-No Estimated
TOTAL		Total-Yes Observed	Total-No Observed	TOTAL $a+b+c+d$

180 In addition, evaluations were also made for the daily TRMM estimates and gauge data, based
 181 on a 2×2 contingency table (Table 2), by detecting rain events, no events, misses by TRMM and false-
 182 alarms by the TRMM, over the Indus river basin.

183 We used a threshold of 0.3 mm/d, to differentiate precipitation and no precipitation events since
 184 lower precipitation values may be the result of noise, as indicated by [30, 38] etc.

185 Based on these four indicators, orders as shown the table, several categorical statistical indices
 186 are derived, including, accuracy (Ac), bias score or frequency bias index (FBI), probability of detection
 187 (POD), false alarm ratio (FAR, critical success index (CSI) and true skill statistics (TSS) [39, 40].
 188 These are defined in the following equations:

189 $Ac = \frac{a+d}{Total}$ (6)

$$190 \quad FBI = \frac{a+b}{a+c} \quad (7)$$

$$191 \quad POD = \frac{a}{a+c} \quad (8)$$

$$192 \quad FAR = \frac{b}{a+b} \quad (9)$$

$$193 \quad CSI = \frac{a}{a+b+c} \quad (10)$$

$$194 \quad TSS = \frac{a}{a+b} - \frac{b}{c+d} = \frac{ad - bc}{(a+b)(c+d)} \quad (11)$$

195 where a represents the number of rainfall events that have been successfully estimated by
 196 TRMM data (hits), b is the number of events incorrectly predicted as rain events by TRMM (false
 197 alarms). c is the number actual events, that are missed by TRMM (Misses), while d is the number of
 198 dry days or no-rainfall events identified successfully by the TRMM dataset. For each day, depending
 199 on how the estimated and observed precipitation behave, any events above the given threshold (0.1
 200 mm), is scored either as hit, miss, false-alarm or correct-negative.so that the rainfall is a hit if both,
 201 TRMM and observed, reach the threshold, False-alarm if if only the TRMM estimate reach the
 202 threshold, miss if only the observed precipitation reaches it, and correct-negative if both are below
 203 the threshold. The number of hits, fals-alarms, misses and correct-negatives ar used in eq-5 to 10, to
 204 calculate the above mentioned statistical indices

205 Each of these indices provides a specific information of the two data sets compared. Thus Ac
 206 indicates the fraction of estimates which is correct (range: 0 to 1. perfect score: 1); FBI indicates
 207 whether the estimated dataset have a tendency to underestimate ($FBI < 1$) or to overestimate ($FBI > 1$)
 208 rain events, POD quantifies the fraction of rain occurrences that is estimated correctly (range: 0 to 1.
 209 perfect score: 1); FAR measures the fraction of false alarms in the satellite rain estimates (perfect score
 210 of 0 and a range from 0 to 1. CSI measures the fraction of estimated events that are correctly predicted
 211 (perfect score: 1) and a range from 0 to 1. Unlike all the aforementioned indices, TSS does not depend
 212 on the frequency of climatological event and uses all elements in the contingency table (Table 2). Thus
 213 TSS provides a measure of the accuracy of the estimates in terms of the probability of correct detection
 214 of events or no events. In this case the range is form -1 to 1. Perfect score is 1, with 0 showing no skills
 215 and a negative score means that the estimates are worse than a random forecast.

216 3. Results and discussion

217 The assessment of the reliability of the TRMM estimates and their comparisons with the rain
 218 data from gauge station presented in this section has been done by three different methodologies, i.e.
 219 (1) a *statistical analysis*, based on R, BIAS, MAE and RMSE for monthly, annual and seasonal data
 220 aggregates, (2) *categorical statistics* daily data by computing Ac , FBI , POD , FAR , CSI and TSS , and (3)
 221 *visual comparison* for monthly, annual and seasonal data.

222 3.1. Statistical analysis

223 The results of the TRMM-assessment based on the statistical measures R , $rBIAS$, MBE , MAE and
 224 $RMSE$, are given for daily data aggregation in **Table 3**, for monthly and annual data aggregation in
 225 Table 4, and for seasonal aggregation in Table 5. The summer season include months of April, May,
 226 June, July, August and September, while the remaining 6 months: October, November, December,
 227 January, February and March are aggregated to represent Winter season.

228 It is evident from a first glance at the two tables that the TRMM performs overall rather poorly
 229 for estimating the observed rain amounts for the study region at all resolutions, as the average R

230 values are only 0.16, 0.22, 0.22 and 0.20 for monthly, annual, and seasonal (summer and winter)
 231 aggregation, respectively. Further specific results are discussed in the subsequent sub-sections

232 3.1.1. Skill Statistics for TRMM precipitation estimates (Daily aggregates)

233 The daily aggregates of TRMM precipitation estimates showed poor skill in matching observed
 234 precipitation, with an average R of 0.16. Our comparison of the observed and TRMM daily rainfall
 235 data shows highly variable MAE across the UIB, with a range ≥ 23 mm/day (Table-3). Values of MAE
 236 were high throughout most of compared locations in UIB, with MAE ≤ 13 mm for the all stations
 237 averaged rainfall, across the UIB. The North-Western parts of the UIB showed the highest and the
 238 most variable MAE. The results showed that the TRMM data have huge under-estimation across most
 239 of the UIB (average MBE of -3.53 mm), while the MBE values also showed a distinct spatial pattern
 240 across the study area, with distinct under-estimation by TRMM estimates for all the studied locations
 241 in the Eastern and Northern UIB; for the Southern UIB, TRMM estimates showed a high under-
 242 estimation at all locations except one; while the stations located in the North-western UIB had a mixed
 243 trend, where TRMM data showed moderate to high, under or over estimation at half (three) of the
 244 locations each. The mean relative bias (rBIAS) at the different gauge location also followed an similar
 245 pattern with huge veriations and ranging from a (-)tive 0.42 to as high as 5.27 (Table 3), while at
 246 certain locations the relative bias was very high and at one location i.e. "Yasin" the rBais was even
 247 more than 5 times the observed values. The RMSE for the daily time series were also very high and
 248 showed large variations, ranging from and 8.08 to as high as 46.57 mm/day, with averages RSME of
 249 20.88 for all locations averaged rainfall.

250 These results are in agreement with previous studies () as most of them have reported TRMM
 251 product to underestimate rainfall amounts over the HKH region in general and even higher over the
 252 western parts of HKH.

253 **Table 3.** Statistical analysis based on monthly and annual data aggregation.

STATION	DAILY				
	R	rBIAS	MBE (mm)	MAE (mm)	RMSE (mm)
Southern UIB	<i>Burzil</i>	0.22	-0.42	-11.77	16.20
	<i>Deosai</i>	0.10	0.99	4.41	14.53
	<i>Rama</i>	0.23	-0.22	-16.20	18.31
	<i>Rattu</i>	0.14	0.69	-7.90	18.12
East ern UIB	<i>Shigar</i>	0.08	1.31	-3.99	10.24
	<i>Hushey</i>	0.14	-0.07	-5.73	10.79
North-Western UIB	<i>Khot</i>	0.19	0.70	0.49	4.93
	<i>Naltar</i>	0.25	0.24	-11.94	15.39
	<i>Shendoor</i>	0.16	1.48	1.22	9.46
	<i>Ushkor</i>	0.21	0.70	-0.51	8.16
	<i>Yasin</i>	0.10	5.27	24.24	28.68
	<i>Zani</i>	0.13	-0.14	-15.23	19.16
Northern UIB	<i>Khunjrab</i>	0.15	-0.27	-5.50	10.52
	<i>Ziarat</i>	0.14	0.71	-0.94	6.05
Average (all stations in UIB)	0.16	0.78	-3.53	13.61	20.88
Maximum	0.25	5.27	24.24	28.68	46.57
Minimum	0.08	-0.42	-16.20	4.93	8.08

255 3.1.2. Skill Statistics for TRMM precipitation estimates (Monthly and annual aggregates)

256 The monthly and annual aggregated TRMM precipitation estimates also showed poor skill in
 257 matching observed precipitation, but with considerably improved values for the Pearson correlation
 258 coefficient R for all the studied locations and with an R of 0.61 and 0.57 for average of rainfall at all
 259 locations for monthly and annual aggregates, respectively.

260 **Table 3.** Statistical analysis based on monthly and annual data aggregation.

	STATION	MONTHLY					ANNUAL				
		R	rBIAS	MBE (mm)	MAE (mm)	RMSE (mm)	R	rBIAS	MBE (mm)	MAE (mm)	RMSE (mm)
Southern UIB	Burzil	0.55	-0.28	-56.80	58.73	112.81	0.43	-1.05	-391.5	391.5	407.7
	Deosai	0.22	0.17	21.65	43.62	78.95	-0.37	0.24	146.6	201.4	234.6
	Rama	0.54	-0.36	-78.26	79.54	165.86	0.78	-2.05	-538.5	538.5	574.8
	Rattu	0.20	-0.20	-39.31	61.32	119.10	0.30	-0.58	-264.9	274.1	353.8
Eastern UIB	Shigar	0.02	-0.21	-19.42	36.56	78.26	-0.11	-0.62	-133.2	179.7	249.8
	Hushey	0.09	-0.24	-29.19	39.72	101.95	-0.15	-0.79	-193.2	230.3	339.6
North-Western UIB	Khot	0.51	-0.21	-26.52	39.47	74.14	0.29	-0.65	-182.0	242.7	250.9
	Naltar	0.60	-0.31	-58.62	60.17	120.63	0.12	-1.32	-395.1	395.1	416.3
	Shendoor	0.42	0.08	6.53	22.08	37.34	0.54	0.13	40.4	66.4	99.1
	Ushkor	0.52	-0.03	-1.82	19.19	39.41	0.62	-0.05	-14.7	79.1	110.5
	Yasin	0.21	1.36	118.35	126.68	241.25	0.10	0.72	806.0	806.0	827.5
	Zani	0.49	-0.34	-75.05	77.98	154.91	0.52	-1.69	-508.3	508.3	532.6
Northern UIB	Khunjrab	0.39	0.05	2.26	13.13	23.40	-0.28	0.09	18.3	52.0	70.0
	Ziarat	0.38	-0.07	-5.39	15.23	32.62	0.55	-0.15	-30.6	73.4	104.7
Average (all stations in UIB)		0.61	-0.23	-9.09	14.15	20.98	0.57	-0.24	-117.3	117.3	134.1
Maximum		0.60	1.36	118.35	126.68	241.25	0.78	0.72	806.03	806.03	827.54
Minimum		0.02	-0.36	-78.26	13.13	23.40	-0.37	-2.05	-538.50	51.96	69.96

261 Our comparison of the observed and TRMM monthly and annual aggregated rainfall also
 262 showed a highly variable MAE across the UIB, ranging from 13.13 mm/month to 126.68 mm/month,
 263 in case of monthly aggregates and from -538.5 mm/year to 806.0 mm/year for annual aggregates
 264 (**Table-4**). The values for MAE were high throughout most of compared locations in UIB, with an
 265 average MAE of 14.15 mm/month and 117.3 mm/year, for the all locations average monthly and
 266 annual rainfall across UIB, respectively. The spatial pattern of the errors observed in case of monthly
 267 and annual aggregates as well as the predominant under-estimation at most location was similar to
 268 that observed for the daily aggregates. The North-Western parts of the UIB showed the highest and
 269 the most variable MAE, while the TRMM data showed huge under-estimation across most of the UIB
 270 (average MBE of a (-)tive 9.09 mm/month and -117.3 mm/year). The Eastern part UIB, showed a
 271 distinct under-estimation by TRMM rainfall, across all the studied locations. In case of the Southern
 272 UIB, the under-estimation was even higher but observed at three out of the four location, while at
 273 one location (Deosai), an over estimation of 21.65 mm/month was observed. The stations located in
 274 the North-western UIB had a mixed trend, where TRMM data showed a moderate to high, under-
 275 estimation at four of the studied locations while the opposite in the remaining two, for both monthly
 276 and annual aggregates. The MBE for the total of two location evaluated in the northern UIB, showed

277 a mixed results with one station (Khunjrab) showing slight over-estimation (0.05 mm/month and 18.3
 278 mm/year), while the other (Ziarat) showing a negative MBE (-0.07 mm/month and -30.6 mm/year).

279 3.1.3. Skill Statistics for TRMM precipitation estimates (Seasonal aggregates)

280 The seasonal statistical indices (Table 4) have comparable trends in terms of magnitude,
 281 however, show a different pattern than the monthly- or annually computed ones. For example the in
 282 summer season the TRMM showed positive BIAS for a few location where the monthly and annual
 283 aggregates show a negative one (i.e. Rattu, Ushkor). Results for the winter season predominantly
 284 show negative BIAS- values, similar to monthly and annual aggregation. The overall range of MBE
 285 for the stations evaluated varies from -268.8 mm to 593.6 mm for the summer season and from -339.9
 286 mm to 212.5 mm for winter season. The MBE for average rainfall across all location in UIB, was -5.18
 287 and -96.51 mm for summer and winter respectively. These MBE value are comparatively lower in
 288 case of summer season, are suggestive of a situation where the under or over-estimation occurring in
 289 the different months of the seasons, cancel each other out to give an overall low MBE.

290 **Table 4. Statistical analysis based on summer and winter season data aggregation**

Regions	STATIONS	SUMMER SEASON					WINTER SEASON				
		R	rBIAS	MBE	MAE	RMSE	R	rBIAS	MBE	MAE	RMSE
				(mm)	(mm)	(mm)			(mm)	(mm)	(mm)
Southern UIB	Burzil	0.35	-0.48	-190.8	190.8	201.5	0.05	-0.50	-200.7	200.7	226.0
	Deosai	-0.42	0.27	68.1	101.0	123.5	-0.14	0.31	78.6	116.9	139.6
	Ramma	0.68	-0.54	-198.7	198.7	213.9	0.60	-0.92	-339.9	339.9	371.4
	Rattu	0.49	0.09	25.8	101.0	127.9	-0.01	-1.00	-290.8	290.8	357.1
Eastern UIB	Shigar	-0.09	-0.22	-36.9	106.0	156.6	-0.10	-0.57	-96.3	105.4	127.9
	Hushey	0.22	-0.35	-83.2	103.7	156.3	-0.55	-0.46	-109.9	132.2	189.3
North-Western UIB	Khot	-0.11	-0.03	-4.1	38.1	48.3	0.33	0.16	22.2	29.2	34.8
	Naltar	0.48	-0.50	-203.8	203.8	220.6	0.17	-0.47	-191.6	191.6	205.9
	Shendoor	0.57	0.42	56.1	56.7	79.6	-0.02	-0.12	-15.9	61.1	65.6
	Ushkor	0.49	0.17	31.0	71.9	84.1	0.65	-0.25	-45.9	55.3	85.7
	Yasin	-0.35	2.94	593.6	593.6	615.2	0.22	1.05	212.5	212.5	244.1
	Zani	0.52	-0.66	-268.8	268.8	301.3	0.57	-0.59	-239.8	239.8	256.1
Northern UIB	Khunjrab	0.09	-0.21	-41.3	91.8	109.2	0.56	-0.72	-141.1	157.5	166.9
	Ziarat	0.56	-0.02	-2.5	36.2	47.4	0.54	-0.20	-28.4	44.8	65.3
	Average (all stations in UIB)	0.60	0.00	-5.18	30.1	38.7	0.36	-0.4	-96.51	96.5	109.1
Maximum		0.68	2.94	593.6	593.6	615.2	0.65	1.05	212.5	339.9	371.4
Minimum		-0.42	-0.66	-268.8	36.2	47.4	-0.55	-1.00	-339.9	29.2	34.8

291 The R ranges showed better values for the summer season (0.6) in comparison to winter season,
 292 for the basin average seasonal aggregates, while it ranged from -0.42 to 0.68 and -0.55 to 0.65 for the
 293 summer and winter seasons respectively.

294 3.2. Categorical statistics

295 The results for the six categorical indices, as described in Section 2.3 are listed in Table 5 and
 296 they show how the TRMM-data match the ground-based gauge data at daily resolution. Thus the
 297 values for the first index, accuracy (*Ac*) are well above 0.50 for all stations, with an average of 0.58.
 298

299 The frequency bias index *FBI* has neither very high positive nor negative values, but varies on
 300 both sides with 9 stations showing overestimation, and the remaining 5 an underestimation. The
 average *FBI* for all stations is 1.05, i.e. indicates a slight overestimation of the TRMM rainfall.

301 The other categorical indices (see Eq. 8-11) do not show very good results either. Thus, for most
 302 of the stations the values of the probability of detection (*POD*) is below 0.5, with only 4 stations having
 303 values above it. The False Alarm Ratio (*FAR*) for all stations, but one, are too high, with an average
 304 of 0.56. In the same way, both the *CSI*- and the *TSS* values are also not very promising as only 3
 305 stations have values above 0.30 for the former and only one station has a value of about 0.20 for the
 306 latter.

307 Thus, overall, these results of the categorical statistics indicate that TRMM rainfall estimates do
 308 not have a very good match with the ground-based gauge data and, therefore, should only be used
 309 after some corrections and adjustments have been made.

310 **Table 5. Categorical statistics for daily TRMM estimate and gauge rain data.**

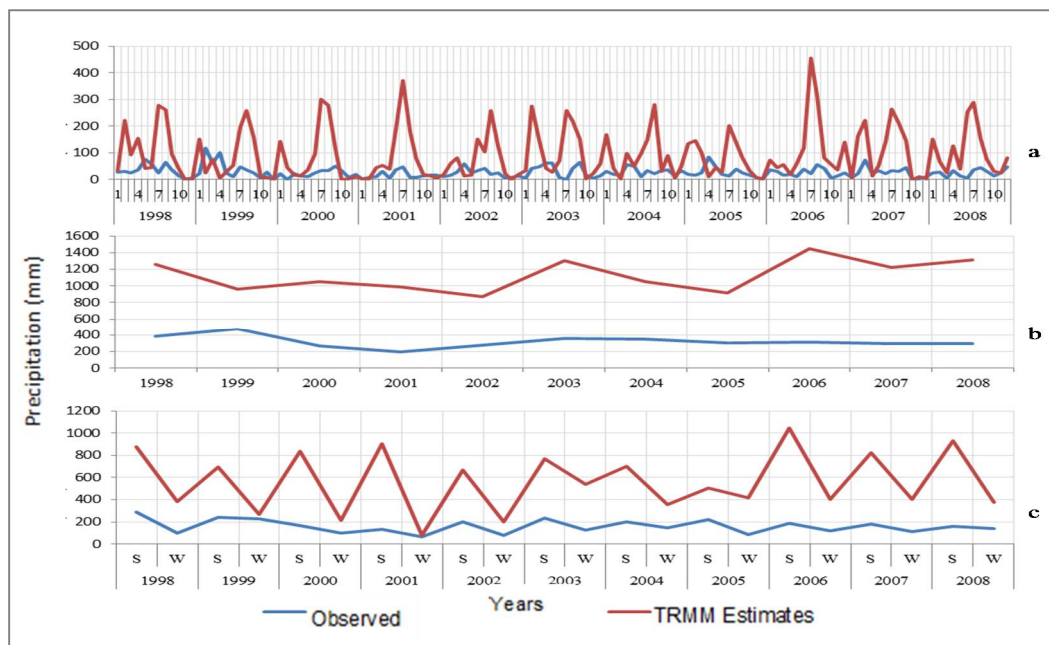
Regions		STATIONS			Ac	FBI	PO D	FA R	CSI	TS S				
Southern UIB		<i>Burzil</i>			0.5	0.7	0.42	0.45	0.3	0.1				
		<i>Deosai</i>			0.5	1.0	0.61	0.39	0.4	0.1				
		<i>Ramma</i>			0.5	1.2	0.50	0.61	0.2	0.0				
		<i>Rattu</i>			0.5	1.4	0.56	0.62	0.2	0.0				
Eastern UIB		<i>Shigar</i>			0.6	1.3	0.41	0.68	0.2	0.0				
					0	0			2	8				
		<i>Hushey</i>			0.5	0.8	0.40	0.52	0.2	0.1				
					7	3	8	0						
North-Western UIB		<i>Khot</i>			0.6	1.3	0.57	0.58	0.3	0.2				
		<i>Naltar</i>			0.6	0.8	0.40	0.53	0.2	0.1				
		<i>Shendoor</i>			0.5	1.1	0.40	0.65	0.2	0.0				
		<i>Ushkor</i>			0.6	1.0	0.42	0.60	0.2	0.1				
		<i>Yasin</i>			0.6	1.0	0.44	0.58	0.2	0.2				
		<i>Zani</i>			0.5	0.8	0.35	0.59	0.2	0.0				
Northern UIB		<i>Khunjrab</i>			0.5	1.0	0.43	0.58	0.2	0.0				
					5	4			7	6				
		<i>Ziarat</i>			0.6	0.7	0.35	0.52	0.2	0.1				
					0	3	5	0						
Average (all stations in UIB)					0.5	1.0	0.45	0.56	0.2	0.1				
Maximum					0.6	1.4	0.61	0.68	0.4	0.2				
Minimum					0.5	0.7	0.35	0.39	0.2	0.0				
Regions	STATION <i>S</i>	Ac	FBI	PO D	FA R	CSI	TS S							

Southern UIB	<i>Burzil</i>	0.5	0.7	0.42	0.45	0.3	0.1
	<i>Deosai</i>	0.5	1.0	0.61	0.39	0.4	0.1
	<i>Ramma</i>	0.5	1.2	0.50	0.61	0.2	0.0
	<i>Rattu</i>	0.5	1.4	0.56	0.62	0.2	0.0
Eastern UIB	<i>Shigar</i>	0.6	1.3	0.41	0.68	0.2	0.0
		0	0			2	8
	<i>Hushey</i>	0.5	0.8	0.40	0.52	0.2	0.1
		7	3			8	0
North-Western UIB	<i>Khot</i>	0.6	1.3	0.57	0.58	0.3	0.2
	<i>Naltar</i>	0.6	0.8	0.40	0.53	0.2	0.1
	<i>Shendoor</i>	0.5	1.1	0.40	0.65	0.2	0.0
	<i>Ushkor</i>	0.6	1.0	0.42	0.60	0.2	0.1
	<i>Yasin</i>	0.6	1.0	0.44	0.58	0.2	0.2
	<i>Zani</i>	0.5	0.8	0.35	0.59	0.2	0.0
Northern UIB	<i>Khunjrab</i>	0.5	1.0	0.43	0.58	0.2	0.0
		5	4			7	6
	<i>Ziarat</i>	0.6	0.7	0.35	0.52	0.2	0.1
		0	3			5	0
Average (all stations in UIB)	0.5	1.0	0.45	0.56	0.2	0.1	
	8	5			8	1	
	0.6	1.4	0.61	0.68	0.4	0.2	
Minimum		0.5	0.7	0.35	0.39	0.2	0.0

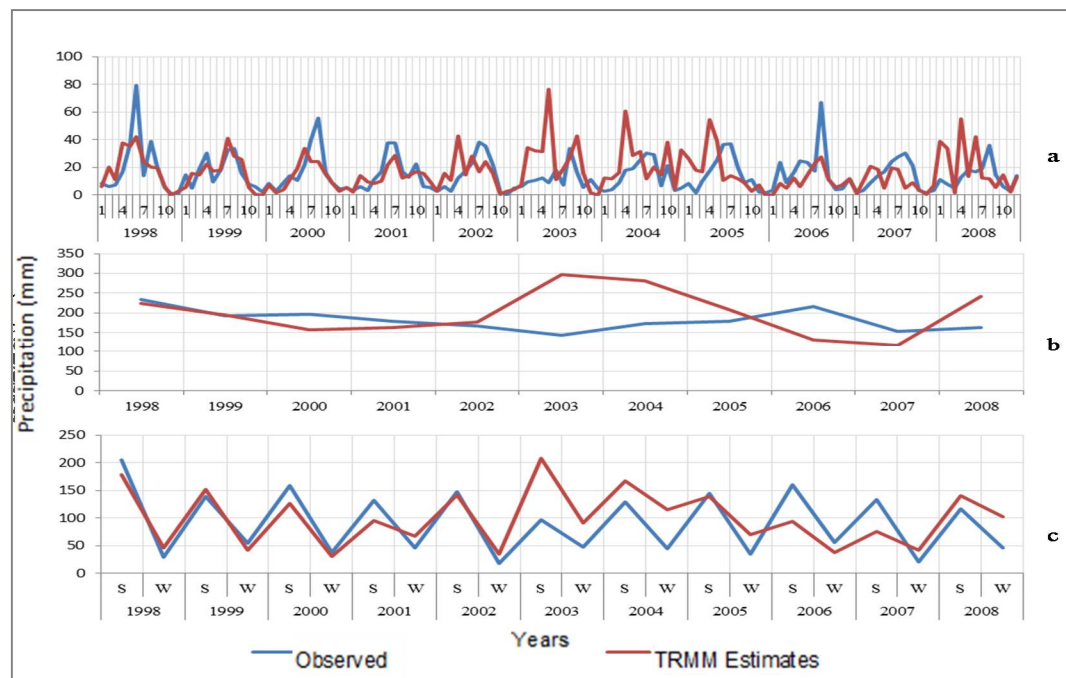
311 3.3. Visual comparison

312 For visual comparison, monthly-, annually- and seasonally aggregated time series of the TRMM-
 313 rainfall estimates and of the various gauge stations are plotted.

314 Figs. 2 and 3 show these time series plots for the two stations Yasin and Khunjrab, respectively.
 315 One may notice that for the station Yasin (Fig. 2) shows huge biases and errors at all three time scales
 316 considers, whereas for the other station Khunjrab, a better match, especially, at the annual and
 317 seasonal resolution is obtained. The corresponding plots for the others stations reveal patterns
 318 somewhere in between the two stations shown here.

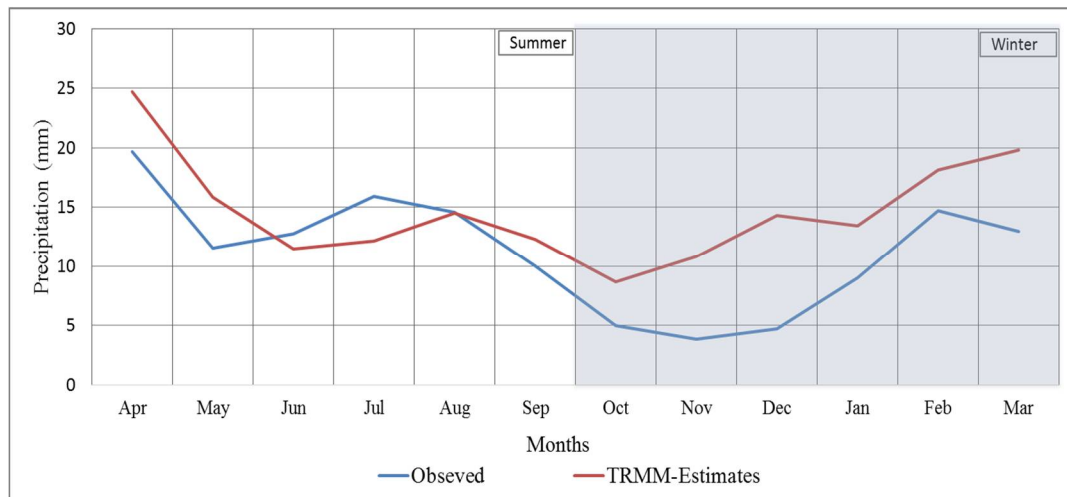


319 **Figure 2:** Time series of TRMM estimates and gauge data for rainfall totals at Yasin station; a.
320 monthly, b. annual, and c. seasonal (S=Summer, W=Winter)



321 **Figure 3:** Time series of TRMM- estimates and observed gauge data for mean rainfall totals at
322 Khunjrab station; a. monthly, b. annual, and c. seasonal (S=Summer, W=Winter)

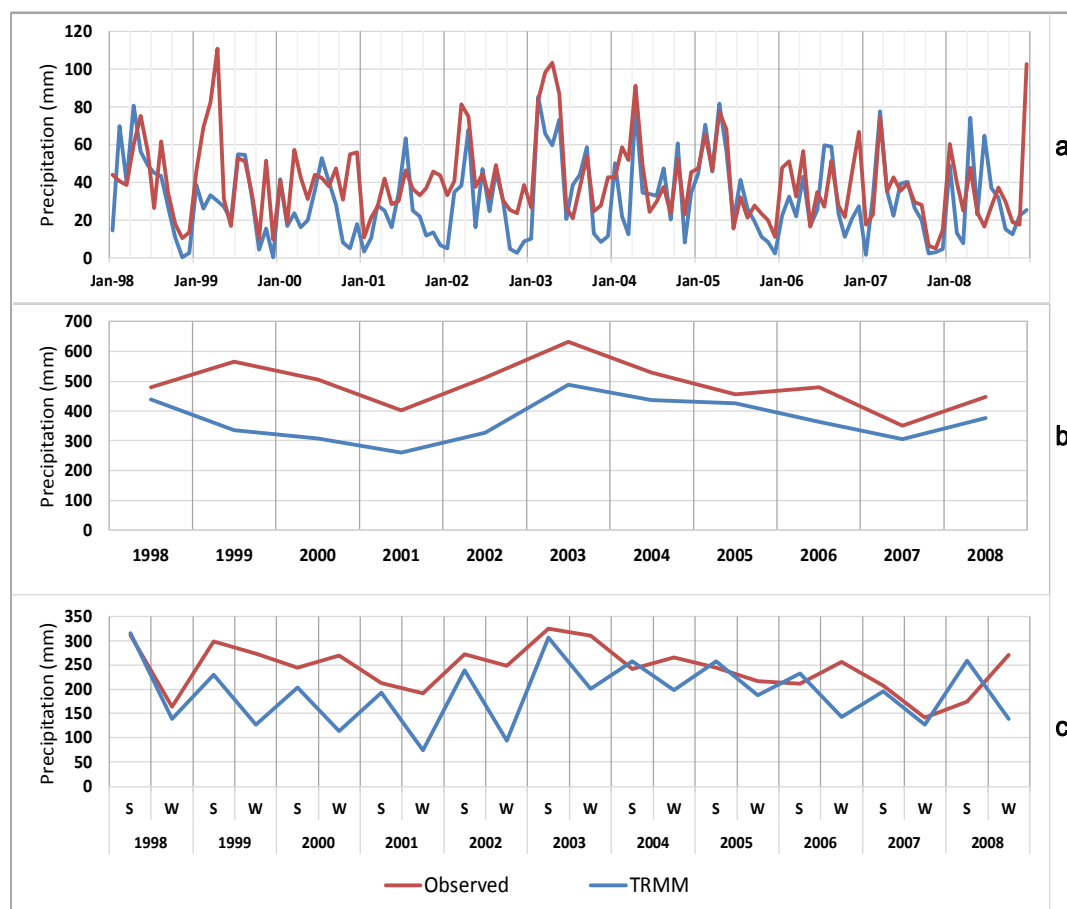
323 The monthly TRMM- and gauge rainfalls averaged over all stations and the full length of period
324 considered (1998–2008), is plotted in Fig. 4. The figure also have demarcation of the seasons. From the
325 figure an underestimation of the TRMM- rainfall in the winter months and a mix of under and
326 overestimation in the summer months can clearly be seen.



327

328 **Figure 4.** Comparison of TRMM-estimates and gauge data for mean monthly rainfall for all stations
 329 with seasonal demarcation.

330 Finally, the monthly-, annually- and seasonally aggregated time series of the TRMM- rainfall
 331 estimates of the average rainfall across all the studied gauge stations are plotted in **Fig-5**. Though
 332 there is almost a persistent underestimation by the TRMM estimates, the peaks and troughs, in most
 333 instances followed similar patterns.
 334



335

336 **Figure 5:** Time series of TRMM- estimates and observed gauge data for mean rainfall totals over
 337 the study area, for all the gauge stations ; a. monthly, b. annual, and c. seasonal
 338 (S=Summer, W=Winter)

339 **4. Discussions and Conclusions**

340 In this study a TMPA product - TRMM 3B42 V7 data for the Upper Indus basin, Pakistan, for
341 the period 1998-2008 has been assessed and evaluated on a point-to-point basis, using rain gauge data
342 from 14 stations. These assessments have been performed at monthly, seasonal and annual
343 aggregation scales. The results indicate that the TMPA product has considerable errors in estimating
344 the rainfall amounts at the various gauge stations throughout the study area and throughout the total
345 time period studied. There is a predominant trend of under- estimation across the study area as at
346 most of the gauge stations, the TRMM product tends to under-estimate the gauge-measured rainfall.
347 The seasonal TRMM- rainfall values, though, show a specific pattern, with the summer rainfall
348 slightly overestimated, but those for the winter predominantly underestimated at almost all locations
349 and all aggregation time scales.

350 These overall results are in conformity of the previous studies, which, in most cases, suggest that
351 neither the sparsely observed station data and gridded data products based on them, nor the sensors
352 based data, fully represent the precipitation regime of the region [41], with strong non-representation
353 or underestimation [16] of regional precipitation amounts, especially for higher altitudes by [41, 20,
354 22]. In fact the *in situ* meteorological observations in UIB are sparse and mostly taken at valley based
355 stations. This data provide low spatial coverage and is scant for higher altitudes. Furthermore, the
356 complex orography of the UIB region also affects the amounts, spatial patterns and seasonality of
357 precipitation. Additionally, most of the authors have indicated that the observation network across
358 the UIB, also show underestimation of precipitation amounts by [20, 22, 41–43], with an average
359 underestimation of around 166%, which may reach even in excess of 300% over some parts of the
360 basin [43]. This means that the TRMM product may even be underestimating the true areal
361 precipitation by a much greater margin, as the true areal precipitation is estimated to be much higher
362 [43] than the gauge observation records.

363 The comparison of any gridded or sensor based dataset against the observed precipitation, may
364 not be taken, therefore, as a conclusive evidence for declaring the evaluated data as unappropriated
365 in terms of usability but rather show the degree to which these data sets match for magnitudes or
366 occurrences with the observed precipitation, which by no means is perfect., and a better match may
367 also indicate the evaluated data also may have tendencies to underestimate the real areal
368 precipitation over the UIB. Furthermore, the resolution of the TRMM product (0.25° X 0.25°), may
369 also pose limitations, especially for distributed hydrological modelling and investigations, as at this
370 resolution, the orographic influences on the precipitation regime cannot be mapped, while the
371 hydrological models may also require precipitation data at a much finer scale.

372 The main conclusion which can be drawn from our study may be summed up as: 1) The TRMM
373 3B42 V7 product has an overall poor agreement with the observed rainfall gauge data in the study
374 area, and this holds for all temporal scales considered; and 2) our results, eventually means that
375 the TMPA-TRMM 3B42 V7 product may only be regarded as suitable for further rainfall analyses and
376 subsequent hydrological applications in the study region, if some improvements, down-scaling and
377 local calibrations of its output data are carried out first.

378

379 **Author Contributions:**

380 Asim Jahangir Khan conceived and designed the experiments, conducted the analysis and is responsible for
381 writing; Manfred Koch helped developing the idea, supervised the analyses and the writing process and he is
382 responsible for parts of the text; Karen Milena Chinchilla is responsible for parts of the statistical analysis and
383 helped developing ideas.

384 **Funding:** "This research received no external funding".

385 **Acknowledgments:** "Tropical Rainfall Measurement Mission Project (TRMM), Daily TRMM and Others Rainfall
386 Estimate (3B42 V7 derived), version 7, data used in this study were produced with the Giovanni online data
387 system, developed and maintained by the NASA GES DISC."

388 **Conflicts of Interest:** "The authors declare no conflict of interest."

389

390 **References**

391

- 392 1. Scheel, M.L.M.; Rohrer, M.; Huggel, C.; Santos Villar, D.; Silvestre, E.; Huffman, G.J. Evaluation of
393 TRMM Multi-satellite Precipitation Analysis (TMPA) performance in the Central Andes region and its
394 dependency on spatial and temporal resolution. *Hydrol. Earth Syst. Sci.* **2011**, *15*, 2649–2663,
395 doi:10.5194/hess-15-2649-2011.
- 396 2. Hasanpour Kashani, M.; Dinpashoh, Y. Evaluation of efficiency of different estimation methods for
397 missing climatological data. *Stoch Environ Res Risk Assess* **2012**, *26*, 59–71, doi:10.1007/s00477-011-
398 0536-y.
- 399 3. Behrang, A.; Khakbaz, B.; Jaw, T.C.; AghaKouchak, A.; Hsu, K.; Sorooshian, S. Hydrologic evaluation
400 of satellite precipitation products over a mid-size basin. *Journal of Hydrology* **2011**, *397*, 225–237,
401 doi:10.1016/j.jhydrol.2010.11.043.
- 402 4. Pegram, G.; Deyzel, I.; Sinclair, S.; Visser, P.; Terblanche, D.; Green, G. Daily mapping of 24 hr rainfall
403 at pixel scale over South Africa using satellite, radar and raingauge data: In: 2nd International Precipitation
404 Working Group (IPWG) Workshop, Naval Research Laboratory, Monterey, USA. 25-28 October **2004**.
- 405 5. Ghile, Y.; Schulze, R.; Brown, C. Evaluating the performance of ground-based and remotely sensed near
406 real-time rainfall fields from a hydrological perspective. *Hydrological Sciences Journal* **2010**, *55*, 497–
407 511, doi:10.1080/02626667.2010.481374.
- 408 6. Oke, A.M.C.; Frost, A.J.; Beesley, C.A. The use of TRMM satellite data as a predictor in the spatial
409 interpolation of daily precipitation over Australia: In: 18th World IMACS/MODSIM Congress, 13-17
410 July **2009**.
- 411 7. Chiew FHS, Vaze J, Viney NR, Jordan PW, Perraud J-M, Zhang L, Teng J, Young WJ, Penaarancibia J,
412 Morden RA, Freebairn. *Rainfall-runoff modelling across the Murray-Darling Basin. A report to the*
413 *Australian Government from the CSIRO Murray-Darling Basin Sustainable Yields ProjectT*; CSIRO,
414 Australia, 2008.
- 415 8. Hughes, D.A. Comparison of satellite rainfall data with observations from gauging station networks.
416 *Journal of Hydrology* **2006**, *327*, 399–410, doi:10.1016/j.jhydrol.2005.11.041.
- 417 9. Joyce, R.J.; Janowiak, J.E.; Arkin, P.A.; Xie, P. CMORPH: A Method that Produces Global Precipitation
418 Estimates from Passive Microwave and Infrared Data at High Spatial and Temporal Resolution. *J.*
419 *Hydrometeor* **2004**, *5*, 487–503, doi:10.1175/1525-7541(2004)005<0487:CAMTPG>2.0.CO;2.
- 420 10. KUBOTA, T.; SHIGE, S.; Hashizume, H.; AONASHI, K.; TAKAHASHI, N.; Seto, S.; HIROSE, M.;
421 TAKAYABU, Y.N.; Ushio, T.; Nakagawa, K.; *et al.* Global Precipitation Map Using Satellite-Borne
422 Microwave Radiometers by the GSMAp Project: Production and Validation. *IEEE Trans. Geosci. Remote*
423 *Sensing* **2007**, *45*, 2259–2275, doi:10.1109/TGRS.2007.895337.
- 424 11. Ushio, T.; SASASHIGE, K.; KUBOTA, T.; SHIGE, S.; Okamoto, K.'i.; AONASHI, K.; INOUE, T.;
425 TAKAHASHI, N.; IGUCHI, T.; Kachi, M.; *et al.* A Kalman Filter Approach to the Global Satellite
426 Mapping of Precipitation (GSMAp) from Combined Passive Microwave and Infrared Radiometric Data.
427 *JMSJ* **2009**, *87A*, 137–151, doi:10.2151/jmsj.87A.137.

428 12. AONASHI, K.; AWAKA, J.; HIROSE, M.; KOZU, T.; KUBOTA, T.; LIU, G.; SHIGE, S.; KIDA, S.;
429 SETO, S.; TAKAHASHI, N.; *et al.* GSMaP Passive Microwave Precipitation Retrieval Algorithm :
430 Algorithm Description and Validation. *JMSJ* **2009**, *87A*, 119–136, doi:10.2151/jmsj.87A.119.

431 13. Turk, F.J. Rohaly, G.D., Hawkins, J. Smith, E.A., Marzano, F.S. Mugnai, A. Levizzani, V. *Meteorological*
432 *applications of precipitation estimation from combined SSM/I, TRMM and infrared geostationary satellite*
433 *data. In book: Microwave Radiometry and Remote Sensing of the Earth's Surface and Atmosphere*; VSP
434 Intl. Sci. Publ. Zeist, pp 353–363, 2000.

435 14. Huffman, G.J.; Adler, R.F.; Bolvin, D.T.; Nelkin, E.J. The TRMM Multi-Satellite Precipitation Analysis
436 (TMPA).: In: Gebremichael M., Hossain F. (eds) *Satellite Rainfall Applications for Surface Hydrology*.
437 Springer, Dordrecht **2010**, 3–22, doi:10.1007/978-90-481-2915-7_1.

438 15. Huffman, G.J.; Bolvin, D.T.; Nelkin, E.J.; Wolff, D.B.; Adler, R.F.; Gu, G.; Hong, Y.; Bowman, K.P.;
439 Stocker, E.F. The TRMM Multisatellite Precipitation Analysis (TMPA): Quasi-Global, Multiyear,
440 Combined-Sensor Precipitation Estimates at Fine Scales. *J. Hydrometeor* **2007**, *8*, 38–55,
441 doi:10.1175/JHM560.1.

442 16. Andermann, C.; Bonnet, S.; Gloaguen, R. Evaluation of precipitation data sets along the Himalayan front.
443 *Geochem. Geophys. Geosyst.* **2011**, *12*, n/a-n/a, doi:10.1029/2011GC003513.

444 17. Amir Khan, A.; Pant, N.C.; Ravindra, R.; Alok, A.; Gupta, M.; Gupta, S. A precipitation perspective of
445 the Hydrosphere-cryosphere interaction in the Himalaya. *Geological Society, London, Special*
446 *Publications* **2018**, *462*, 73–87, doi:10.1144/SP462.2.

447 18. Hussain, S.; Song, X.; Ren, G.; Hussain, I.; Han, D.; Zaman, M.H. Evaluation of gridded precipitation
448 data in the Hindu Kush–Karakoram–Himalaya mountainous area. *Hydrological Sciences Journal* **2017**,
449 *62*, 2393–2405, doi:10.1080/02626667.2017.1384548.

450 19. Cheema, M.J.M.; Bastiaanssen, W.G.M. Local calibration of remotely sensed rainfall from the TRMM
451 satellite for different periods and spatial scales in the Indus Basin. *International Journal of Remote Sensing*
452 **2012**, *33*, 2603–2627, doi:10.1080/01431161.2011.617397.

453 20. Yatagai, A.; Kamiguchi, K.; Arakawa, O.; Hamada, A.; Yasutomi, N.; Kitoh, A. APHRODITE:
454 Constructing a Long-Term Daily Gridded Precipitation Dataset for Asia Based on a Dense Network of
455 Rain Gauges. *Bull. Amer. Meteor. Soc.* **2012**, *93*, 1401–1415, doi:10.1175/BAMS-D-11-00122.1.

456 21. Palazzi, E.; Filippi, L.; Hardenberg, J. von. Insights into elevation-dependent warming in the Tibetan
457 Plateau-Himalayas from CMIP5 model simulations. *Clim Dyn* **2017**, *48*, 3991–4008, doi:10.1007/s00382-
458 016-3316-z.

459 22. Wijngaard, R.R.; Lutz, A.F.; Nepal, S.; Khanal, S.; Pradhananga, S.; Shrestha, A.B.; Immerzeel, W.W.
460 Future changes in hydro-climatic extremes in the Upper Indus, Ganges, and Brahmaputra River basins.
461 *PLoS ONE* **2017**, *12*, e0190224, doi:10.1371/journal.pone.0190224.

462 23. Wilheit, T.T. Some Comments on Passive Microwave Measurement of Rain. *Bull. Amer. Meteor. Soc.*
463 **1986**, *67*, 1226–1232, doi:10.1175/1520-0477(1986)067<1226:SCOPMM>2.0.CO;2.

464 24. Janowiak, J.E.; Joyce, R.J.; Yarosh, Y. A Real-Time Global Half-Hourly Pixel-Resolution Infrared
465 Dataset and Its Applications. *Bull. Amer. Meteor. Soc.* **2001**, *82*, 205–217, doi:10.1175/1520-
466 0477(2001)082<0205:ARTGHH>2.3.CO;2.

467 25. Ali, K.F.; Boer, D.H. de. Spatial patterns and variation of suspended sediment yield in the upper Indus
468 River basin, northern Pakistan. *Journal of Hydrology* **2007**, *334*, 368–387,
469 doi:10.1016/j.jhydrol.2006.10.013.

470 26. Hewitt, K. Hazards of melting as an option: Upper Indus Glaciers, I&II. *DAWN*, May 20, 2001.

471 27. Tahir, A.A.; Chevallier, P.; Arnaud, Y.; Neppel, L.; Ahmad, B. Modeling snowmelt-runoff under climate
472 scenarios in the Hunza River basin, Karakoram Range, Northern Pakistan. *Journal of Hydrology* **2011**,
473 *409*, 104–117, doi:10.1016/j.jhydrol.2011.08.035.

474 28. Immerzeel, W.W.; van Beek, L.P.H.; Bierkens, M.F.P. Climate Change Will Affect the Asian Water
475 Towers. *Science* **2010**, *328*, 1382–1385, doi:10.1126/science.1183188.

476 29. Wake, C.P. Glaciochemical Investigations as a Tool for Determining the Spatial and Seasonal Variation
477 of Snow Accumulation in the Central Karakoram, Northern Pakistan. *A. Glaciology*. **1989**, *13*, 279–284,
478 doi:10.3189/S0260305500008053.

479 30. Hewitt, K. Glacier Change, Concentration, and Elevation Effects in the Karakoram Himalaya, Upper
480 Indus Basin. *Mountain Research and Development* **2011**, *31*, 188–200, doi:10.1659/MRD-JOURNAL-D-
481 11-00020.1.

482 31. Ali, S.; Li, D.; Congbin, F.; Khan, F. Twenty first century climatic and hydrological changes over Upper
483 Indus Basin of Himalayan region of Pakistan. *Environ. Res. Lett.* **2015**, *10*, 14007, doi:10.1088/1748-
484 9326/10/1/014007.

485 32. Hasson, S.u. Future Water Availability from Hindu Kush-Karakoram-Himalaya upper Indus Basin under
486 Conflicting Climate Change Scenarios. *Climate* **2016**, *4*, 40, doi:10.3390/cli4030040.

487 33. Singh, P.; Kumar, N. Effect of orography on precipitation in the western Himalayan region. *Journal of
488 Hydrology* **1997**, *199*, 183–206, doi:10.1016/S0022-1694(96)03222-2.

489 34. Dhar, O.N.; Rakhecha, P.R. The effect of elevation on monsoon rainfall distribution in the central
490 Himalayas. In *Monsoon dynamics*; Lighthill, M.J., Pearce, R.P., Eds.; Cambridge University Press: New
491 York, 1981; pp 253–260.

492 35. Dahri, Z.H.; Ludwig, F.; Moors, E.; Ahmad, B.; Khan, A.; Kabat, P. An appraisal of precipitation
493 distribution in the high-altitude catchments of the Indus basin. *Science of The Total Environment* **2016**,
494 *548-549*, 289–306, doi:10.1016/j.scitotenv.2016.01.001.

495 36. Pang, H.; Hou, S.; Kaspari, S.; Mayewski, P.A. Influence of regional precipitation patterns on stable
496 isotopes in ice cores from the central Himalayas. *The Cryosphere* **2014**, *8*, 289–301, doi:10.5194/tc-8-
497 289-2014.

498 37. Archer, D. Contrasting hydrological regimes in the upper Indus Basin. *Journal of Hydrology* **2003**, *274*,
499 198–210, doi:10.1016/S0022-1694(02)00414-6.

500 38. Mayor, Y.G.; Iryna Tereshchenko, Mariam Fonseca-Hernández; Diego A. Pantoja; Jorge M. Montes.
501 Evaluation of Error in IMERG Precipitation Estimates under Different Topographic Conditions and
502 Temporal Scales over Mexico. *Remote Sensing* **2017**, *9*, 503, doi:10.3390/rs9050503.

503 39. Wilks, D.S. *Statistical methods in the atmospheric sciences. An introduction*; Acad. Press: San Diego,
504 1995.

505 40. Wilks, D.S. *Statistical Methods in the Atmospheric Sciences*, 3. Aufl.; Elsevier/Academic Press:
506 Amsterdam, 2011.

507 41. Palazzi, E.; Hardenberg, J. von; Provenzale, A. Precipitation in the Hindu-Kush Karakoram Himalaya:
508 Observations and future scenarios. *J. Geophys. Res. Atmos.* **2013**, *118*, 85–100,
509 doi:10.1029/2012JD018697.

510 42. Palazzi, E.; Filippi, L.; Hardenberg, J. von. Insights into elevation-dependent warming in the Tibetan
511 Plateau-Himalayas from CMIP5 model simulations. *Clim Dyn* **2017**, *48*, 3991–4008, doi:10.1007/s00382-
512 016-3316-z.

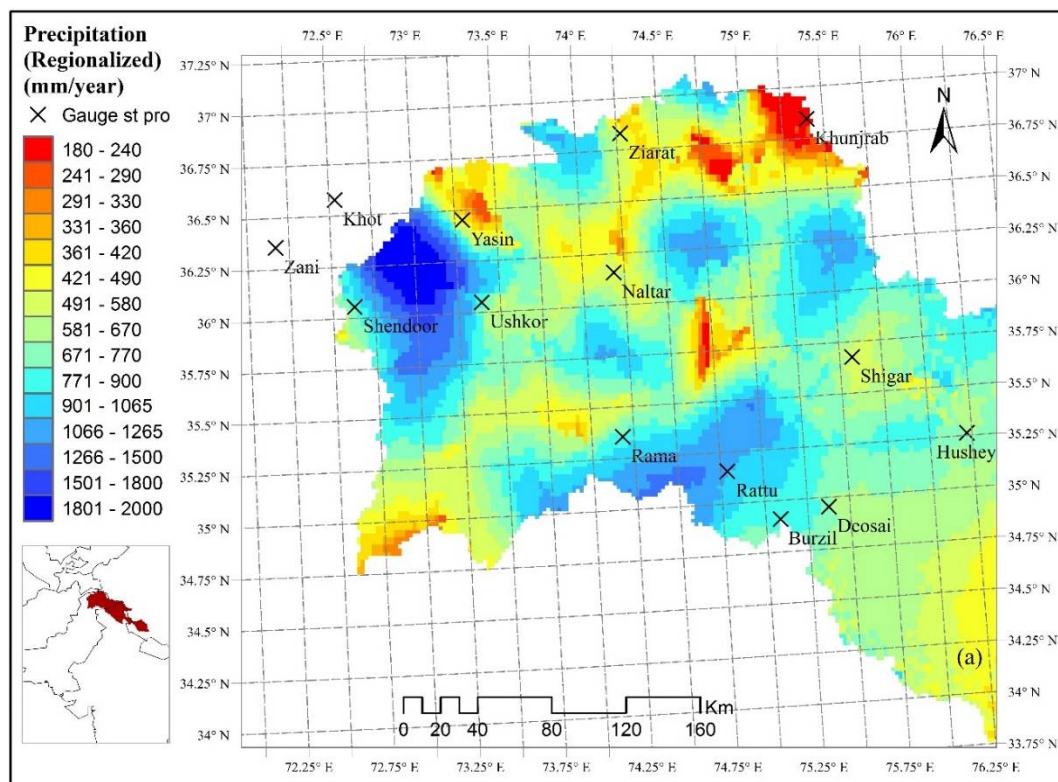
513 43. Khan, A.J.; Koch, M. Correction and informed regionalization of precipitation data in a high
514 mountainous region (Upper Indus Basin) and its effect on SWAT-modelled discharge **2018 (un**
515 **published)**.

516

517

Appendices-Supplementary Materials

App.I : Spatial Precipitation regimes in UIB (adopted from Khan and Koch unpublished)



App.II Vertical meteorological and cryospheric regimes in UIB (modified from Hewitt 2007)

